Static and Dynamic Analysis of Airships

Jong-ho Woo* and V. R. Murthy†
Syracuse University, Syracuse, New York

Consideration of geometric nonlinearities is important in the static and dynamic design of nonrigid airships. The finite-element method, using MSC/NASTRAN, is applied to perform linear and nonlinear static analyses and to determine the free vibration characteristics of such airships. It is found that the solutions obtained using the linear plus differential stiffness matrix may be quite adequate for airship structural analysis. A procedure to design a wrinkle-free catenary curtain is presented. The necessary solution sequence alterations used to determine the natural vibration characteristics of airships using MSC/NASTRAN are presented.

Nomenclature

A = cross-sectional area, ft^2
c_ℓ = lift coefficient of helium
E = modulus of elasticity, lb/ft^2
E_{11}, E_{22} = modulus of elasticity along principal material axes, orthotropy is assumed, lb/ft^2
F = vector of element forces, lb
G = shear modulus, lb/ft^2
K = incremental stiffness matrix
P = vector of applied loads, lb
p = pressure loading, lb/ft^2
Q = vector of forces of constraint, lb
t = nominal thickness, ft
U = displacement vector, ft
w = weight density, lb/ft^3
x,y,z = right-handed cartesian coordinate system, x-axis positive bow to stern, z-axis positive vertically up
ν_{12}, ν_{21} = Poisson's ratios

Introduction

DURING the last few years, there has been an upsurge in airship developmental activities, due to new transport, maritime patrol, and airborne area surveillance requirements. The activities started with an interagency workshop on lighter-than-air vehicles, conducted in Monterey, California.[1] These were followed by several government and privately sponsored studies to define the vehicle concepts and their potential applications.[2,3] For one reason or another, these efforts did not go beyond feasibility analyses.

The advent of sea-skimming missiles, including Soviet cruise missiles, has created a very strong need for a long-endurance, organic, airborne platform from which to conduct area surveillance and communication as well as command and control operations.[4] The U.S. Navy has identified the airship as the potential platform to meet this new requirement. A few months ago, the Navy issued a request for proposal (RFP) for an airship with operational testing scheduled to take place before 1991.

Airship technology has not progressed to the level of the heavier-than-air flight systems, due to a lack of significant developmental activities during the last three decades. Therefore, it is important to apply the recent advances in basic flight system technologies to airships. In the flight dynamics area, pioneering work is being done by Nagabhushan et al.[5-11] at Goodyear Aerospace. In the present paper, the finite-element method is applied to static structural and free vibration analyses of airships. In a recent paper,[12] a linear finite-element analysis using MSC/NASTRAN was performed to determine the stresses in aerostats. In this paper, however, a nonlinear finite-element analysis is performed to determine the structural behavior of airship envelopes compared with the linear solution, both obtained using MSC/NASTRAN. Also, for the first time free vibration characteristics of airship envelopes are computed. These play an important role in response analyses due to dynamic loads, and in the dynamic design of hybrid lighter-than-air systems.[5-11]

The present study concludes that:

1) MSC/NASTRAN is a very convenient program to perform static and dynamic analyses of airships;

2) the solutions obtained using the linear elastic plus differential stiffness matrix are quite adequate for airship analyses; and

3) differential stiffness and added masses have a significant effect on the dynamic characteristics of airships.

Method of Solution

The airship is modeled using the triangular membrane and rod elements of MSC/NASTRAN. The first iteration of the nonlinear solution is the generation of the linear solution assuming the displacements to be small. The second iteration corresponds to the differential stiffness solution. The term differential stiffness applies to linear terms in the equations of motion of an elastic body that rises from a simultaneous consideration of large, nonlinear motions and the applied loads. It is assumed in the theory of differential stiffness that rotations and strains are small. The Lagrangian discrete element approach is used to calculate the differential stiffness matrix. The approach involves these steps: 1) calculation of the internal forces due to the applied loads assuming the displacements to be small (linear theory); 2) calculation of the work done by the internal forces due to the movement of their point of applications, assuming the internal forces to be constant both in magnitude and direction; and 3) once the work done is known, the stiffness matrix can be obtained by the application of the Lagrange's equations of motion.

The solution algorithm of the nonlinear problem is an extension of the differential stiffness approach. All the assumptions of the theory of differential stiffness are applicable here. The approach requires a displaced element coordinate system to be constructed for each element, which follows and rotates with the element as the model deforms. Changes in shapes of the element (distortions) are treated as displacements with respect to the displaced element coordinate system. Rigid body displacements and rotations do not contribute to the distortions. In the displaced element coordinate system, the

Received Feb. 26, 1987; revision received July 20, 1987.

*Graduate Student, Department of Mechanical and Aerospace Engineering.

†Associate Professor, Department of Mechanical and Aerospace Engineering. Member AIAA.

distortions are small, and linear elastic theory can be used. Element forces in the displaced element coordinate system are computed by simply premultiplying the displacements by the (small motion) elastic stiffness matrix. The incremental stiffness matrix, when expressed in the displaced element coordinate system, is the sum of the elastic and differential stiffness matrices. Applied loads are computed using the displaced geometry, which allows the inclusion of follower-type forces in the model.

The recurrence relation corresponding to the modified Newton-Raphson procedure employed in MSC/NASTRAN is given by

$$[K^m]\{U^{n+1} - U^n\} = \{P^\ell - F^n + Q^{n+1}\} \quad (1)$$

where n = loop counter; ℓ = last loop when loads were updated; and m = last loop when matrices were updated. Equation (1) is used only for the third and successive iterations.

Thus, the solution sequence is an iterative procedure as previously discussed. Each iteration is defined by the analyst through a subcase in the case control deck (defined in the user's manual of MSC/NASTRAN). The first subcase defines the linear static analysis and the second subcase defines a differential stiffness analysis. All additional subcases will use the full geometric nonlinear capability. In addition to specifying the number of iterations to be performed through the number of subcases provided, the analyst may control the calculation within each subcase. The significant calculations are:

1) Recalculation of $[K^m]$ in Eq. (1) can be skipped for selected iterations in order to reduce the number of calculations. However, skipping matrix operations will increase the number of iterations needed for solution. In the present problem $[K^m]$ is regenerated for every iteration. This implies that $m = n$ in Eq. (1).

2) Load calculations can be skipped when the loads are not being incremented and are not functions of displaced geometry. In the present problem, the entire load is applied in one step and all subsequent load calculations are skipped. This implies that $\ell = 1$ in Eq. (1).

The analyst should be familiar with the design and construction of nonrigid airships for successful completion of nonlinear finite-element analyses. The design and construction of the outer shell of a basic nonrigid airship is based on a single-compartment gas hull. The hull is pressurized to a sufficient level at which it can carry all the loads without wrinkling. Its major structural components are here described.

Envelope

This is the outer shell of the airship and is usually constructed in the panels and gores employing polyester fabrics coated with neoprene. The fineness ratio is usually in the range of 3.8 to 4.8 and its (envelope) shape corresponds to a standard equation. This shape can be known as unrigged shape. The initial finite-element model corresponds to this shape. The stresses in the fabrics are usually expressed in terms of load per unit width, rather than per unit area. This is because the thickness is not known with much precision and also is often irrelevant due to the fact that fabrics derive their strength from the yarns.

Suspension System

The purpose of the suspension system is to transfer uniformly the loads from the car to the envelope. There are two kinds of suspension systems in the airship structure: 1) internal suspension system, and 2) external suspension system. The internal suspension system is the main load-carrying system and consists of catenary curtain and cables. The top portion of the curtain is sewn to the envelope and the cables connect the car to the curtain. Several small external catenary systems are used to position the car firmly against the envelope and a fairing encloses the external cables to reduce drag and provide envelope/car integrity. The shape of the curtain and the pretensions in the catenary cables are designed such that they (catenary curtain and as well as cables) remain under tension at all loading conditions. This pretensioning load condition is called the rigging condition and the associated cable tensions are known as "rigging tensions." These rigging tensions are introduced into the cables by shortening them, and this pulls the car firmly against the pressurized envelope; this provides structural integrity for the envelope/car. Thus, the surface of the envelope that is in contact with the car will be flat, and this condition is imposed in the finite-element analysis by means of "car top pressure."

Nose Battens

The nose stiffening is achieved by means of a nose cone and battens. The purpose of the nose stiffening is twofold: 1) to prevent buckling of the nose, and 2) to transfer the ground mooring loads to the envelope.

As mentioned earlier, the fabric panels are cut to a standard initial shape and the finite-element model is prepared based on this shape. The rigged shape of the envelope is then the deformed shape obtained as a result of applying the following loads to the initial geometry: 1) pressure loading, including buoyancy; 2) gravity loading (weights); 3) car top pressure; and 4) rigging tensions.

The rigged shape and the associated stresses are computed for the following three cases: 1) elastic (linear) stiffness matrix; 2) elastic plus differential stiffness matrix; and 3) nonlinear stiffness matrix.

The free vibration characteristics assuming small vibratory motions from the rigged shape are computed using the MSC/NASTRAN program. Since the airship is a lighter-than-air system, the virtual masses associated with the acceleration dependent fluid forces are important. These are computed in NASTRAN and added to the physical masses. The eigenvalues are extracted by first tridiagonalizing the dynamic stiffness matrix by the modified Given's method and later by extracting the eigenvalues of the tridiagonal matrix by the QR-transformation.

Description of the Model

Airship Data

The airship data given in Table 1 is assumed for numerical calculations.

Material Properties

Material properties for fabrics employed for hull, catenary curtains, and empennage should be determined from tests. Since the test data for actual airship fabrics are not available, the material properties given in Table 2 for the envelope and catenary curtains are assumed (orthotropic):

Finite-Element Model and Boundary Conditions

A vertical plane of symmetry is assumed, and one-half of the airship envelope is divided into 168 triangular elements. The

Table 1 Airship data

Volume	180,000 ft^3
Ballonet volume	45,000 ft^3
Length	160 ft
Maximum diameter	45 ft
Pressure at the airship centerline	15.6 lb/ft^2
Location of the center of gravity (C.G.) from the nose	77.5065 ft
Location of center of buoyancy from the nose	77.5097 ft
Weight of the envelope	640.881 lb
Weight of the catenary system	23.0425 lb
Weight of the empennage	400 lb
Lift coefficient of the helium	0.0635

Table 2 Material Properties

Properties for envelope and catenary curtains (orthotropic):

$E_{11} = 2.9479 \times 10^4$ lb/ft^2
$E_{22} = 2.4566 \times 10^4$ lb/ft^2
$\nu_{12} = 0.032888$
$\nu_{21} = 0.039465$
$G = 2.04 \times 10^3$ lb/ft^2
$w = 10$ oz/yd
t = nominal thickness of unity, 1 ft

Properties for catenary cables (isotropic):

$E = 4.32 \times 10^9$ lb/ft^2
$G = 1.66 \times 10^9$ lb/ft^2
$w = 5.2530 \times 10^2$ lb/ft^2
$A = 5.0 \times 10^{9-4}$ ft^2

Properties for nose battens (isotropic):

$E = 1.45 \times 10^9$ lb/ft^2
$G = 5.59 \times 10^8$ lb/ft^2
$w = 1.693 \times 10^2$ lb/ft^3
$A = 4.224 \times 10^{-3}$ ft^2

Table 3 Cable rigging tensions

Cable no.	Cable rigging tensions, lb
1	1.256×10^6
2	6.060×10^5
3	5.717×10^5
4	5.395×10^5
5	4.008×10^5
6	4.626×10^5
7	4.599×10^5
8	1.351×10^6

catenary curtain is divided into 15 triangular elements. There are 14 rod elements in the one half of the model: six for the nose battens and eight for the catenary cables. The finite-element model is shown in Fig. 1, and altogether there are 109 nodes. The x-z plane is assumed to be a plane of symmetry and therefore y-displacements in this plane are assigned zero values. The model is constrained in all degrees of freedom at nodes 48 and 62, where the internal suspension system is attached to the car.

Due to lack of design details, the external suspension system is not included in the model. This implies that the internal suspension system carries 100% of the load. The empennage and car structures are not treated as part of the envelope structure.

Rigging Loads

The following loads are applied to determine the rigged shape of the envelope:

1) Pressure loading, including buoyancy:

$$P = P_o + c_\ell z$$

2) Gravity loading, in which actual weights are calculated and applied at the appropriate locations;

3) Force due to pressure on the car top, 400 lb/ft; and

4) Rigging tensions in the cables of the internal suspension system, as shown in Table 3.

In real life situations, the rigging tensions are specified by the design, and the finite-element analysis has to be performed in an iterative fashion to realize the desired tensions. In the present case the above tensions are assumed based on preliminary design.

Numerical Results and Discussion

The finite-element model of the airship is shown in Fig. 1. The model has 109 nodes with the following elements: 1) 168 triangular elements for the envelope, 2) 15 triangular elements for the catenary curtain, 3) 8 rod elements for the catenary cables, and 4) 6 rod elements for the nosebattens.

The model is very coarse, and the degrees of freedom are intentionally kept low to have a reasonable turnaround time on the IBM 4341 computer, which is a relatively small machine. In a commercial environment, 600 to 700 nodes are recommended and will yield very accurate results. The solutions obtained for the model shown in Fig. 1 are given in Tables 4–6 for the following three cases:

1) *Linear stiffness*—This case corresponds to the classical linear elastic case with small displacements assumption;

2) *Linear plus differential stiffness*—This case includes the stiffness of case 1 as well as the linear terms that arise from the considerations of work done by the external forces due to the large displacements of their points of application;

3) *Nonlinear stiffness*—This case corresponds to the large displacement problem solved by the modified Newton-Raphson method after 18 iterations.

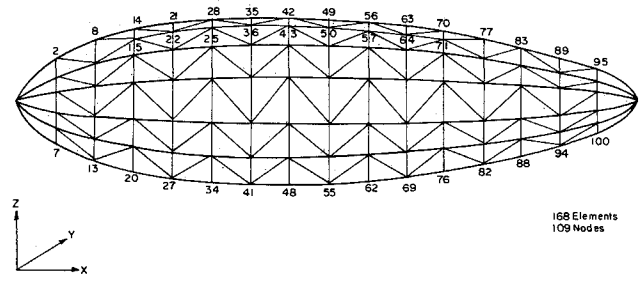

Fig. 1a Finite element model for the envelope.

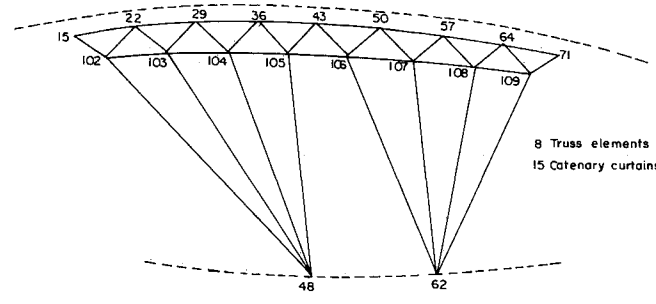

Fig. 1b Model for the internal suspension system.

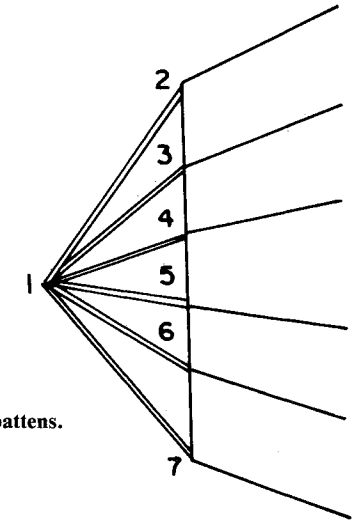

Fig. 1c Model for the nose battens.

Table 4a Comparison of deflections, along x-axis, ft

Grid no.	Linear stiffness	Linear plus differential stiffness	Nonlinear stiffness
42	4.8669×10^{-2}	5.4926×10^{-2}	5.9895×10^{-2}
43	4.7164	5.3502	5.8348
44	3.8870	4.5423	4.9928
45	1.8270	2.5748	2.8853
46	0.4650	0.8310	1.0035
47	−0.1914	−0.1400	−0.0772
48	0.0	0.0	0.0

Table 4b Comparison of deflections, along y-axis, ft

Grid no.	Linear stiffness	Linear plus differential stiffness	Nonlinear stiffness
42	0.0×10^{-2}	0.0×10^{-2}	0.0×10^{-2}
43	−5.8792	−5.8260	−5.8718
44	−20.6380	−19.1913	−19.2000
45	−49.2030	−38.3088	−38.9875
46	−32.1963	−31.7117	−31.5511
47	−11.0372	−14.6988	−14.2751
48	0.0	0.0	0.0

Table 4c Comparison of deflections, along z-axis, ft

Grid no.	Linear stiffness	Linear plus differential stiffness	Nonlinear stiffness
42	4.6218×10^{-2}	5.3042×10^{-2}	5.5430×10^{-2}
43	2.2227	3.0360	3.3476
44	13.6359	12.5759	12.9971
45	20.6389	11.4009	12.4451
46	8.4142	−0.7419	0.3253
47	8.4626	−3.3582	−2.0995
48	0.0	0.0	0.0

In all of the above cases, the entire rigging load is applied in a single step, and the nonlinear solution is converged in about 14 iterations based on strain energy considerations. The stiffness matrix is regenerated within each iteration. The variation of strain energy with iterations is given in Table 7.

It is to be noted that the strain energy given in Table 7 is associated with the incremental displacements but not with the total displacements. The total vertical rigging load applied to the model, based on the undeformed geometry, is 2678 lbs. The total of the vertical forces at nodes 48 and 62, which are the only points constrained in the z-direction, is 2766. The difference between the applied load and the reactive load is approximately 3% and can be attributed partly to the change in the volume of the envelope due to stretching. The pressure load is reapplied within each iteration normal to the deformed geometry of the element, and the total load is given by the pressure multiplied by the stretched area. The remaining difference, if any, can be reduced by choosing a finer mesh and applying the load in several increments rather than in a single step.

The strains in the present problem are assumed to be small, implying that the material obeys the linear stress-strain laws. The material properties for the envelope and catenary curtain are assumed to be orthotropic. The stress levels of the airship fabrics under normal operating conditions are well within the linear range and, hence, this assumptions is quite valid for present applications.

The deflections along the x, y, and z directions at approximate grid locations corresponding to the maximum diameter are given in Table 4. The x-axis is taken as positive from bow to stern, the z-axis is positive upwards, and x,y,z forms a cartesian

Table 5a Comparison of stresses; major principal, lb/ft^2

Grid no.	Linear stiffness	Linear plus differential stiffness	Nonlinear stiffness
64	344	343	345
66	334	334	336
68	315	318	317
70	316	315	315
72	310	308	309
74	318	312	312
76	345	344	346
78	333	336	335
80	316	318	318
82	318	318	317
84	311	308	309
86	301	298	299

Table 5b Comparison of stresses; minor principal, lb/f

Grid no.	Linear stiffness	Linear plus differential stiffness	Nonlinear stiffness
64	108	117	117
66	141	146	146
68	190	180	180
70	171	176	174
72	131	143	142
74	141	135	135
76	110	119	119
78	139	144	144
80	189	180	180
82	178	183	182
84	146	156	155
86	98	97	98

Table 5c Comparison of stresses; maximum shear, lb/ft^2

Grid no.	Linear stiffness	Linear plus differential stiffness	Nonlinear stiffness
64	118	113	114
66	96	94	95
68	63	69	69
70	72	70	70
72	90	85	84
74	89	88	89
76	117	112	113
78	97	95	96
80	63	69	69
82	70	68	68
84	82	76	77
86	102	101	101

right-handed coordinate system. The airship finite-element model consisting of membrane elements is not stable before it develops the geometric stiffness. To overcome this problem, a small amount of bending stiffness is given to each membrane element, and the stresses developed due to bending are small compared to the membrane stresses. In real life analyses, the stresses due to bending can also be eliminated, if desired, by dropping the bending stiffness after the geometric stiffness is incorporated into the problem. The deflections shown in Table 4 correspond to the rigged shape because these solutions are obtained by applying the rigging loads as: 1) pressure loading, including buoyancy; 2) gravity loading (weights); 3) car top pressure; and 4) rigging tensions. The major and minor principal and maximum shear stresses associated with the rigged shape are shown in Table 5. From the results shown in Tables 4 and 5, it can be seen that the linear plus differential stiffness case gives reasonably accurate results. This accuracy will be quite satisfactory even during the detailed design phase.

Table 6 Comparison of natural frequencies, Hz

Mode no.	Without added mass			With added mass		
	Linear stiffness	Linear elastic plus differential stiffness	Nonlinear stiffness	Linear stiffness	Linear elastic plus differential stiffness	Nonlinear stiffness
1	0.68912	7.89572	7.92042	0.13310	0.77628	0.77668
2	1.58122	9.09787	9.17549	0.22269	1.87007	1.86787
3	2.76446	9.38413	9.38220	0.41181	2.02670	2.02618
4	2.91789	9.45358	9.45879	0.55053	2.26833	2.26695
5	3.28931	9.90274	9.86830	0.65889	2.38890	2.39253
6	3.36370	10.02452	9.99057	0.68925	2.44743	2.43875
7	9.65966	10.82742	10.72310	0.93552	2.62153	2.62115
8	4.04761	11.27711	11.31399	0.99669	2.67311	2.67323
9	4.23949	11.75881	11.77909	1.04679	2.98679	2.98535
10	4.34639	11.98739	12.05673	1.20089	3.11026	3.11281

One of the authors of this paper has considerable experience with the validation of the finite-element analysis of Goodyear's GZ-20 airship envelope using a custom-tailored, nonlinear finite-element program named SHELL, developed at Goodyear with the assistance of Battelle Laboratories in Columbus, Ohio. Although not verified, the present results, obtained using MSC/NASTRAN, may be comparable to the SHELL results, and the comparison will be an interesting exercise. The convergent nonlinear solutions for airship type of structures can be generated within a day, using NASTRAN after the model is ready, by an expert in finite-element analysis; it will be very time-consuming and tedious to generate comparable convergent solutions, using SHELL. Even though the SHELL program may give very accurate results, MSC/NASTRAN can be used very effectively to design the airship structures.

The airship model employed in the present paper is hypothetical; hence, the design details for the internal catenary curtain are not available. The finite-element analysis is used to design the catenary curtain so that it is free from wrinkles due to the rigging loads. A reasonable shape and size is assumed for the catenary curtain to create the finite-element model. At the end of the linear analysis, several wrinkles can be observed in the curtain, and a set of nonuniform negative temperatures are applied for thermal contraction of the elements so that the curtain will remain in tension during the subsequent nonlinear iterations. Once the temperature loading is established, the following procedure can be used for the design of the curtain:

1) Calculate the stresses in the curtain with and without the temperature loadings;

2) Calculate the differences in the stresses of both problems solved in step 1 and convert them to statically equivalent nodal loading, or simply recover the data of internal nodal forces and calculate their differences;

3) Calculate the enforced displacements needed to generate the differential nodal loading calculated in step 2; and

4) Determine the initial shape of the curtain to be fabricated by subtracting the displacements calculated in step 3 from the deformed shape of the curtain obtained with the temperature loading.

In all of these steps, the rigging loads should be fully effective. All of the above calculations can be done very conveniently in MSC/NASTRAN, and there may not be any need to go beyond the linear plus differential stiffness case. In the actual design process, one has to consider the application of flight loads to the rigged airship. Either linear analysis or, at the most, linear plus differential stiffness analysis may be quite satisfactory to calculate the stresses associated with the flight loads.

Determination of the free vibration characteristics is an important part of the dynamic design. The dynamic loading considerations are particularly important for hybrid airships, such as the quad-rotor helistat, and also for conventional airships, which can encounter unusual dynamic loadings due to suspended structures. Airships are lighter-than-air systems; hence, acceleration-dependent air forces (usually known as added mass forces) have to be taken into account. The free vibration characteristics of the airship structure under consideration are presented in Table 6 for two cases: one with and the other without the added masses. Again, three subcases, viz., linear stiffness, linear plus differential stiffness, and nonlinear stiffness are considered for each case. The following observations can be made from the results presented in Table 6:

1) Added mass forces have significant effect on the natural frequencies;

2) Differential stiffness is extremely important to predicting the natural frequencies; and

3) Incremental stiffness beyond the differential stiffness does not have any appreciable effect.

The added mass forces are calculated, using the MSC/NASTRAN procedures, and no attempts have been made to validate these procedures. In future studies, it is planned to validate the procedures for the exterior flow problems. Typical solution sequence alters, and case-control decks to calculate the natural frequencies and the mode shapes are given in the Appendix for ready use.

Table 7 Variation of strain energy with iterations

Iteration no.	Strain energy, lb-ft
14	1.1×10^{-10}
15	3.6×10^{-10}
16	2.6×10^{-10}
17	1.1×10^{-10}
18	4.6×10^{-11}

Conclusions

The nonlinear static analysis of the MSC/NASTRAN program is applied to determine the rigged shape of nonrigid airship. Each iteration is defined by the analyst through a subcase in the case control deck. The first two subcases correspond to linear static and differential stiffness analyses, respectively. The nonlinear solution is converged in about 14 iterations. It is found that the differential stiffness solution (second subcase) is quite satisfactory for airship analyses.

The free vibration characteristics of the airship envelope are computed for two cases: one with and the other without the added masses. Again, three subcases, viz., linear stiffness, linear plus differential stiffness, and nonlinear stiffness are considered for each case. The conclusions are as follows:

1) effect of added masses is significant;

2) differential stiffness is extremely important; and

3) incremental stiffness beyond the differential stiffness does not have any appreciable effect.

Appendix

a. Alter to Store Stiffness Matrix

```
NASTRAN PREFOPT = 2
ID NONLINEAR SOLUTION
SOL 64
DIAG 8
ALTER XXX
MATPRN      STIFF// $
OUTPUT4     STIFF//-1/35 $
ENDALTER
CEND
LOAD = n
SUBCASE 1
SUBCASE n
BEGIN BULK
```

b. Alter to Calculate Frequencies and Mode Shapes

```
NASTRAN PREFOPT = 2
ID NATURAL FREQUENCY
SOL 63
DIAG 8
ALTER XXX
JUMP ABC $
ALTER XXX
LABEL ABC
INPUTT4     /STIFF, , , , /1/34/3/1 $
ADD         KXX,STIFF/KSTIFF $
READ        KSTIFF,MMAA,MR,DMX,EED,
            VXCOMPR,CASES/LAMA,
            PHIX,MI,OEIGS/V,N,
            READAPP/S,N,NEIGV $
ENDALTER
CEND
METHOD = n
MFLUID=n
LOAD = n
DISPL = ALL
SEALL = ALL
SVECT = ALL
BEGIN BULK
```

References

[1]Vittek, J. E. (Ed.), *Proceedings of the Interagency Workshop on Lighter-Than-Air Vehicles*, Massachusetts Inst.of Technology Rept. FTL-R 75-2, Jan. 1975.

[2]Anonymous, "Study of Civil Markets for Heavy Lift Airships," Booz-Allen Applied Research, NASA, CR-152202, Dec. 1978.

[3]Bailey, D. B. and Rappoport, H. K., "Maritime Patrol Airship Study (MPAS)," Naval Air Systems Command Rept. NADC-80149-60, March 1980.

[4]Anonymous, "A New Mission for an Old Standby," Hughes Aircraft Co., *Vectors*, Vol. 28, No. 1, 1986.

[5]Nagabhushan, B. L. and Tomlinson, N. P., "Flight Dynamics Simulation of Heavy Lift Airship," *Journal of Aircraft*, Vol. 18, Feb. 1981, pp. 96–102.

[6]Nagabhushan, B. L. and Tomlinson, N. P., "Dynamics and Control of a Heavy Lift Airship Hovering in a Turbulent Cross Wind," *Journal of Aircraft*, Vol. 19, Oct. 1982, pp. 826–830.

[7]Nagabhushan, B. L., "Dynamics Stability of a Buoyant Quad-Rotor Aircraft," *Journal of Aircraft*, Vol. 20, March 1983, pp. 243–249.

[8]Nagabhushan, B. L. and Faiss, G. D., "Thrust Vector Control of a V/STOL Airship," *Journal of Aircraft*, Vol. 21, June 1984, pp. 408–413.

[9]Nagabhushan, B. L. and Tomlinson, N. P., "Thrust Vectored Takeoff, Landing, and Ground Handling of an Airship," *Journal of Aircraft*, Vol. 23, March 1986, pp. 250–256.

[10]Nagabhushan, B. L., Lichty, D. W., and Tomlinson, N. P., "Control Characteristics of a Buoyant Quad-Rotor Research Aircraft," *Journal of Guidance and Control*, Vol. 6, March-April 1983, pp. 91–99.

[11]Nagabhushan, B. L., Jacobs, P. P., Belknap, C., and Euler, D. A., "Performance Characteristics of Buoyant Quad-Rotor Research Aircraft," *Vertica*, Vol. 7, No. 3, 1983, pp. 209–223.

[12]Hunt, J. D., "Structural Analysis of Aerostat Flexible Structure by the Finite-Element Method," *Journal of Aircraft*, Vol. 19, Aug. 1982, pp. 674–678.